Journal of Applied Polymer Science

# Variable-Emittance Infrared Electrochromic Skins Combining Unique Conducting Polymers, Ionic Liquid Electrolytes, Microporous Polymer Membranes, and Semiconductor/Polymer Coatings, for Spacecraft Thermal Control

**Prasanna Chandrasekhar,[1] Brian J. Zay,[1] David Lawrence,[1] Edmonia Caldwell,[2] Rubik Sheth,[3] Ryan Stephan,[3] John Cornwell[3]**

[1]Ashwin-Ushas Corporation, Marlboro, New Jersey 07746

[2]National Aeronautics and Space Administration (NASA) - Goddard Space Flight Center (NASA-GSFC), Greenbelt, Maryland 20771

[3]NASA-Johnson Space Flight Center (NASA-JSFC), Houston, Texas 77058

Correspondence to: P. Chandrasekhar (E-mail: chandra.p2@ashwin-ushas.com)

**ABSTRACT:** Variable emittance ($\varepsilon$) is a property vital for the increasing needs in thermal control of future microspacecraft. This article describes fabrication, function, and performance of thin-film, flexible, variable-emittance (V-E) electrochromic skins that use a conducting polymer/-Au/-microporous membrane (CP/Au/μP) base, and a new, unique ionic liquid electrolyte (IonEl). Poly(aniline-co-diphenyl amine) with a long-chain polymeric dopant is used as the CP. A unique, patented device design yields no barrier between the active, electrochromic CP surface and the external environment, except for a thin, infrared-transparent semiconductor/polymer film that lowers solar absorptance [$\alpha(s)$] and protects from atomic-O/far-UV. Use of the IonEl requires special activation methods. Data presented show tailorable $\varepsilon$ variations from 0.19 to 0.90, $\Delta\varepsilon$ values of $>0.50$ (which is the highest reported thus far for any functional V-E material, to our knowledge), $\alpha(s) < 0.35$, and nearly indefinite cyclability. Extended space durability testing, including calorimetric thermal vacuum and continuous light/dark cycling over >7 months under space conditions ($<10^{-5}$ Pa vacuum, far-UV), show excellent durability. Other data show resistance to solar wind, atomic-O, electrostatic discharge, and micrometeoroids. These lightweight, inexpensive, advanced polymeric materials represent the only technology that can work with micro- (<20 kg) and nano- (<2 kg) spacecraft, thus eventually allowing for much greater flexibility in their design and potentially "democratizing" the entire space industry, for example, allowing small firms to launch their own, dedicated satellites. © 2014 Wiley Periodicals, Inc. J. Appl. Polym. Sci. **2014**, *131*, 40850.

**KEYWORDS:** applications; conducting polymers; electrochemistry; ionic liquids; optical and photovoltaic applications

Received 24 February 2014; accepted 12 April 2014

**DOI: 10.1002/app.40850**

## INTRODUCTION

### Infrared Electrochromics

Advanced materials capable of large, dynamic (switchable, controllable) variation of infrared (IR) signature continue to be intensely sought for two major applications: (1) military camouflage countermeasures against IR cameras.[1–7] (2) Spacecraft thermal control,[2,8–11] as discussed in this article. In this respect, electrochromics based on conducting polymers (CPs) have been the subject of much interest, as they have shown electrochromic activity in the visible through microwave regions.[2,12–18] When incorporated into practical devices, electrochromics may be either transmission-mode, with the modulated light beam transmitted through the device or material (e.g., as in windows), or reflectance-mode, with the modulated light beam reflected from the device or material (e.g., as in mirrors). Practical IR signature variation is achieved only with reflectance-mode devices.[2]

### Spacecraft Thermal Control and Variable-Emittance Materials

Efficient thermal control is an extremely essential, if unpublicized and uncelebrated, requirement for all spacecraft.[2,8–11] One of the reasons for this is that radiation is the only means of thermal transfer in space (convection and conduction being unavailable). When facing the sun, a spacecraft must reflect as well as emit heat; when facing away from the sun, it must conserve heat. Such transitions, involving an immediate temperature differential of up to 200°C or more, sometimes occur in a matter of tens of seconds (e.g., with spacecraft rotation). Components such as electronics and fluids/hydraulics have a limited temperature of operation, intolerant of such variations and

must thus be protected from them. Large spacecraft have hitherto successfully used conventional thermal control means, such as mechanical louvers[8]; however, such methods are inapplicable to newer micro- (<ca. 20 kg) and nano- (<ca. 2 kg) spacecraft, due to their weight/bulk.[19–23] They are also increasingly inadequate for the greater thermal control needs of modern, energy-intensive, large spacecraft. These latter include future manned missions where multiple coolant loops interface to crew quarters on one end and external radiators (e.g., louvers) on the other.[24–29]

Due to this inadequacy, microspacecraft and nanospacecraft essentially have no means of thermal control today, severely limiting their design. If efficient thermal control means could be found for such small spacecraft, it may revolutionize small spacecraft design and democratize the entire space industry, for it would allow small firms to launch their own, dedicated satellites without having to share transponder or other space with other firms on large satellites.

The determining property of the performance of thermal control materials is emittance ($\varepsilon$), which is emissivity integrated over the spectral range of thermal interest, about 2–45 μm.[30–32] Emissivity describes, roughly, the ability of a material to give out heat, comparing it to the ability of a black body at the same temperature.[30–32] Emittance varies from 0 to 1, with, for example, white Teflon® and black conductive tape typically having emittances, respectively, of about 0.05 and 0.93 [roughly, emissivity = absorptance = (1 − reflectance)[30–32]]. In space use, IR electrochromics are given the appellation variable-emittance (V-E) materials. For space use, V-E materials, in the form of coatings or skins, are generally proposed to be mounted to the external surface of spacecraft or space structures.

Another, important property of thermal control materials is their solar absorptance, $\alpha(s)$, which is an absorptance that is integrated specifically over the solar spectrum,[24–32] with predominant contributions in the 0.3–1.5 μm spectral region. It again varies from 0 to 1, with low values indicating low absorption of solar radiation.

Efficient spacecraft thermal control ideally requires an emittance variation ($\varepsilon$) between 0.80 and 0.10, with a delta ($\Delta\varepsilon$) of 0.40 or more. The benchmark $\varepsilon$ variation is that set by mechanical louvers, 0.15–0.55 ($\Delta\varepsilon$ ca. 0.4).[2,8–12,24–29] Additionally, in an ideal thermal control material, $\alpha(s)$ should remain constantly low, preferably <0.4, while $\varepsilon$ is concomitantly varied from about 0.1 to 0.8, as needed, with $\Delta\varepsilon > 0.4$. That is to say, the absorption of solar radiation by the surface should remain constantly low, while its ability to emit thermal radiation is modulated and varies, ideally between 0.1 and 0.8. Since $\alpha(s)$ and $\varepsilon$ work in very different spectral regions, this is frequently hard to achieve simultaneously. An additional requirement for V-E technologies, including those based on CPs, is the ability to successfully operate under space conditions, which include extreme temperatures (at minimum +/− 100°C), solar wind, radiation, occasional micrometeoroids and, most importantly, high vacuum ($<10^{-5}$ Pa).

A very large number of newer materials and technologies have been studied recently for spacecraft thermal control, all with limited or no success.[33–44] These include, for example: electrostatic systems; phase change materials; microelectromechanical systems; electrophoretics; metal-oxide-based electrochromics; and thermochromics. All have suffered from various drawbacks that have prevented their successful implementation thus far, generally showing poor emittance variation and poor space durability.[33–44]

### Breakthroughs Enabling Practical V-E Materials for Spacecraft Thermal Control

Several years ago, we described an IR electrochromics system, an offshoot of a military IR camouflage technology, with some promise for space application, which used poly(aniline)-based CPs and unique dopants that imparted enhanced IR electrochromism,[2,12,24–38,45–48] and presented a number of advantages over other CP-based electrochromic systems.[49–58] This system, however, had a number of drawbacks that eventually prevented its successful implementation in space. (1) It used gel or semisolid electrolytes incapable of operating in space vacuum, requiring a cumbersome hermetic seal with an IR-transparent CsI window that frequently failed or distorted in the vacuum of space. (2) Its high-emittance state was also highly absorptive [$\alpha(s) > 0.80$], leading to severe overheating in sun-facing situations. (3) The gel or semisolid electrolytes also possessed poor thermal conductivity, leading to poor transmission of heat from the spacecraft to the external environment in the high-emittance state. (4) The top, IR-transparent surface displayed poor electrostatic discharge (ESD) properties, especially important in space.

The current communication presents several breakthroughs in the (now patented[59]) technology that overcome all the above drawbacks of the prior-generation technology.[2,45–48] (1) Use of unique room-temperature ionic liquid electrolytes (IonEls) incorporated intimately into the CP matrix, which allows excellent functioning in high vacuum and extreme temperatures of space without the need for seals of any kind (organic IonEls, essentially "room temperature molten salts," have, besides good conductivity no observable vapor pressure and typical liquidus ranges of (−)80 to (+)100°C). (2) Use of a unique, IR-transparent, conductive, well-adhering, highly solar-reflective semiconductor coating, applied to the top surface, that drastically reduces the $\alpha(s)$, limiting it to a range <0.40, while at the same time having no effect on emittance. (3) Use of a single-membrane substrate, with working (active electrochromic CP) and counter (also CP) electrodes on opposite sides of a single microporous membrane. The resulting V-E skins are extremely thin (<0.3 mm) and flexible, and can be cut with scissors to any size/shape. This approach may be contrasted with that of "dual-polymer" electrochromic devices based on CPs.[49–58] (4) Removal of electrochromically inactive, "dead" material from the CP matrix using unique (now patented[59]) electrochemical/thermal methodologies; this led to greatly enhanced high/low emittance contrast, above the benchmark threshold $\Delta\varepsilon = 0.40$. The resulting V-E skins have now passed all applicable space-qualification tests. It is noted in particular that the implementation of the IonEls in our electrochromic skins was not straightforward: It was found that they required unique activation steps before they functioned at all with the CPs, as we describe at length in the sequel in this communication. This may be

expected in view of the well-established properties of IonEls,[60–66] but it is in marked contrast to prior studies describing use of IonEls as electrolytes in electrochromic devices that do not use microporous or other membranes or polymeric substrates.[67–71]

As a final, introductory point, it is respectfully noted that we report herein applied electrochromic polymers, which are now actively deployable in a specific application, namely spacecraft thermal control. These are based on a unique applied-polymer technology, with a [CP/Au/μP/Au/CP] construction base (μP = microporous membrane). This same polymer technology, with a CP/μP-polymer base, has found application in areas as diverse and unrelated as electro-osmotic water vapor transport[72] and voltammetric electrochemical sensors.[73] Additionally, we note that although these developments were achieved a few years ago, issues of government classification and intellectual property protection prevented their reporting earlier; these issues have now been resolved, and we are, thus, now free to report these very promising results here.

## EXPERIMENTAL

### Materials, Skin Components, Device (Skin) Assembly, and Activation

**Materials, Electrode Substrates, and Electropolymerization.** Microporous membrane substrates, of pore size from 0.1 to 0.4 μm, comprising poly(sulfone) and polycarbonate, were procured from Pall Gelman Laboratories, Osmonics, and other vendors. Au was deposited on these via e-beam thermal evaporative deposition to a thickness of about 500 nm. This Au/membrane comprised the electrode substrate, on which the CP was electrochemically polymerized. The electropolymerization (deposition) solution comprised aniline and diphenyl amine monomer (Sigma-Aldrich Chemical Co.), in 95%/5% molar proportion, to a concentration of 0.22*M*, in 0.5*M* sulfuric acid (Sigma-Aldrich) and 0.6*M* dopant [potassium salt of poly(anetholesulfonate) and its analog with pendant sulfate groups (Sigma-Aldrich)], as described in more detail elsewhere,[2,12–18,45–48] Electropolymerization was performed potentiostatically in 3-electrode mode at +1.2 V versus Pt quasi-reference, using an AMTEK Princeton Applied Research (PARC) Model 263 potentiostat/galvanostat, or, occasionally, a Bioanalytical Systems (BAS) Model PWR-3 potentiostat. The thickness of the CP/dopant layer was monitored coulometrically and lay between 0.25 and 2.0 μm. Potential sweep methods for electropolymerization gave slightly poorer results than constant-potential methods, as we reported earlier,[12,14,48,59] and were, thus, not pursued further. Following electropolymerization, the substrates were washed with deionized (D.I.) water and dried. These finished substrates comprised the working (front, electrochromically active) and counter (back) electrodes in devices; the thickness of the CP on the back electrode was generally 5× the thickness on the front electrode. A unique formulation of ionic liquids, as described in more detail elsewhere,[59] was used as the IonEl. This included 1-(2-hydroxyethyl)−3-methylimidazolium bis(trifluoromethylsulfonyl)imide (HEMIM-BTFOI or "NTF2"), *n*-butyl methyl imidazolium tetrafluoroborate (BMIM-BF4 or "BB") and added $LiBF_4$ salt; these were procured from Sigma-Aldrich, Alfa Aesar Chemicals or EMD Chemicals, and were desiccated for 48 h at 55°C in vacuum of $10^{-7}$ Torr ($1.33 \times 10^{-5}$ Pa), although it was found that this did not affect the performance of the V-E skins and so was not really necessary (a total of 27 different IonEls and combinations were screened, as discussed under Results and Discussion).

***Flexible outer layer and α(s)-reduction-coating thereon.*** Space-qualified ultralow-outgassing (ULO) polyethylene (PE), thickness 2 mil (50 μm), was procured from Texas Technologies and Southern Film Extruders. An alternative method of production of extremely thin (<5 μm) ULO-PE was based on published spin-coating methods[74] and was as follows (in square brackets). This is briefly outlined between square brackets here: [Dissolve 2 mil ULO PE in toluene (1.5% w/w) at ∼100°C over ∼1 h. Set spin coater at 1000 RPM. Place 7 mil (175 microns) Mylar disk over stage comprising 25-mil thick, 15-cm diameter. Al plate. Spin PE on Mylar. PE film is readily removable from Mylar substrate and measures out at about 5 μm or less (Mylar + PE= 165 μm, Mylar 160 μm)]. The α(s) lowering and ESD-eliminating coating comprised Ge, indium tin oxide (ITO), Si, and $MgF_2$.[75–78] Prior to deposition of this on the PE films they were cleaned with a brief Ar ion etch. They were then mounted on a rotating dual-stage planetary arrangement. The ITO and doped Ge were deposited using variations of standard, published procedures.[75–78] Dopants tested and used for Ge included S, Se, Sn, Te, Mg, Li, Mn, Cd, and Be and combined in some cases with other materials such as GaAs, GaAlAs, ZnS, ZnSe, and ZnO.[75–78] It was found that ITO coating thicknesses of 7–10 nm were ideal; thinner coatings yielded inadequate surface conductivity (required for anti-ESD properties) and thicker coatings invariably led to melting or damage of the PE in addition to reduced IR transmission. Ge-coating thicknesses between 30 and 50 nm were found to impart the best α(s) properties. This outer layer (doped-Ge–Si/PE) was heat bonded directly to the CP surface of the front (electrochromically active) electrode (cf. Figure 1 under Results and Discussion).

***Charging (loading) of the IonEl into the electrochromic skin.*** The loading of the IonEl into the electrochromic device (skin) was nontrivial: simple filling of the device with the liquid IonEl did not achieve access of the IonEl to the body of the CP or its penetration into the microporous membrane, and resultant devices were not electrochemically or electrochromically active. Rather, a complex, patented[59] "activation" procedure needed to be used to obtain functional electrochromic devices, as described in detail elsewhere[59] and very briefly described here as follows: the IonEl was first allowed to wick up into the micropores of the CP/Au/microporous membrane substrate over a period of 10–48 h at about $10^{-3}$ Torr (0.133 Pa) at 60–85°C. The full electrochromic device (skin) was then assembled. This was then suspended horizontally on a Mylar backing and a voltage of (−)1.25 V was applied to the working electrode (in 2-electrode mode) with a potentiostat, corresponding to the fully reduced state of the CP. Hot air, of temperature 200°C +/− 10°C, was directed to the Mylar backing, and the temperature at the top, working electrode monitored with a thermocouple. The device was then switched multiple times using slight overvoltages (+/− 200 mV applied for tens of ms at a time) over a period of about 30 min. The combination of the heat,

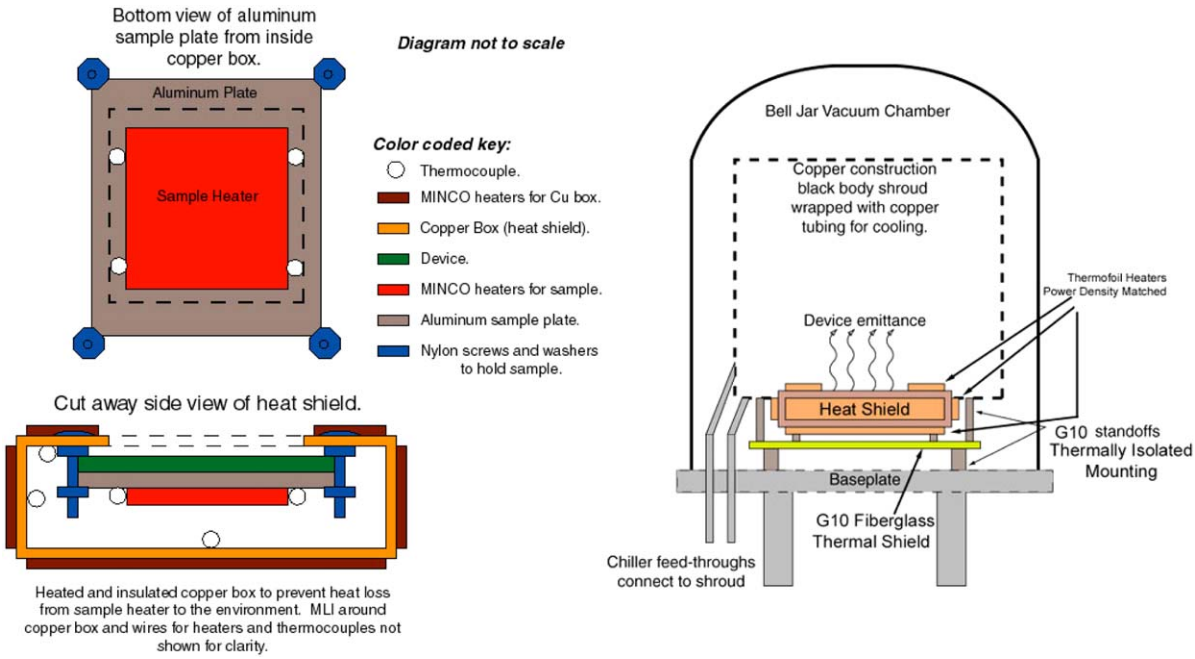


**Figure 1.** Schematic of calorimetric thermal vacuum measurement setup (MLI = multilayer insulation, Device = V-E electrochromic skin). [Color figure can be viewed in the online issue, which is available at wileyonlinelibrary.com.]

applied voltage, and subsequent multiple switching caused the device to activate, with its visual color in the light state changing to gold, corresponding to the fully reduced, transparent state of the polymer. Analyses of the CP matrix on the working electrode for a device thus assembled and activated, using a variety of methods, indicated that: (1) the counterions from the IonEl, for example, $BF_4^-$ and bis(trifluoromethylsulfonyl)amide, had been incorporated into the CP matrix. (2) The IonEl had also been incorporated into the polymer matrix, causing an increase in volume of the matrix of about 25%. It was observed, following the above activation procedures, that the electrochromic skins then switched readily and rapidly (switching time <5 s), at all temperatures and pressures, even down to (−)40°C in high vacuum ($10^{-7}$ Torr, $1.3 \times 10^{-5}$ Pa), whereas, prior to the above activation procedures, they switched very poorly at ambient temperature and pressure and not at all at low temperature and in high vacuum.

***Treatment to remove electrochromically inactive material; V-E skin (device) activation.*** The CP as produced above was found to contain a significant proportion of material that was electrochromically inactive.[59] Thus, as the next step, a patented high-temperature + electrochemical cycling method was used to remove electrochromically inactive portions from the CP matrix on the electrode, as described in more detail elsewhere.[59] To describe this procedure very briefly here, the temperature of the fully assembled skin minus the flexible outer layer was maintained at about 80°C +/− 10°C, while the working electrode was maintained at (−)1.25 V for a period of about 20 min. The electrochromically inactive components of the polymer on the working electrode were dislodged as a result of these actions, and were then physically removed using a latex boom combined with a jet of IonEl applied with a syringe, all the while maintained the (−)1.25 V. The working electrode was then switched between about (−)1.25 and (+)0.5 V multiple (up to 20) times, with residence times at each limit of 60 s, when the current decayed to a steady value, while simultaneously continuing to apply hot air of temperature about 80°C +/− 10°C. The hot air was then removed and the electrode again switched between (−)1.25 and (+)0.5 V multiple (up to 20) times, with residence times at each limit of 60 s. The residual electrochromically inactive components of the polymer on the working electrode were physically removed using the latex boom combined with a jet of ionic liquid applied using a syringe. The skin was then rinsed copiously with D.I. water, dried, and then recharged with IonEl as described in the previous paragraph. It was then ready for application of the flexible outer layer through heat bonding.

## Characterization

**Electrochemical, Spectral Data.** Cyclic voltammograms (CVs) were used for preliminary characterization of skins under varying conditions of temperature and pressure, using a Princeton Applied Research (PARC) Model 263 potentiostat controlled by a PC using PARC's 270/250 software (for 2-electrode-mode work, the reference and counter electrode terminals were shorted together and used as the counter electrode). All reflectance measurements were in situ, as a function of applied potential, which was applied by the above potentiostat in the 2-electrode mode. When appropriate, specular (16° incidence) and diffuse IR reflectance measurements were performed, respectively, on a Perkin–Elmer (P–E) Model Spectrum One FTIR and Bio-Rad FTS 6000 FTIR spectrometer. UV–vis–near-IR (NIR) reflectance was done on a P–E Model Lambda 12. Mirrors or Au surfaces, as appropriate, which were supplied by the vendors, were used as references. For the study of switching time, a "time drive" feature of the FTIR instrument was used, which scanned every 5.2 s and automatically computed the mean %R, with the V-E device itself switched between light

(low-emittance) and dark (high-emittance) states every 60 s (data shown in Figure 7).

***Emittance, solar absorptance measurements.*** Emittance measurements at ambient pressure (and ambient or other temperatures, as appropriate) were performed on an AZ Technology Model TEMP 2000A emissometer (2.5–45 μm range) under active potentiostatic control. Emittance measurements under space vacuum (also at ambient or other temperatures, as appropriate) were performed using calorimetric thermal vacuum methodology (an industry-standard methodology used in the space industry),[79–83] as briefly described in the next paragraph, since the emissometer could not be accommodated in even large high vacuum bell jars. Solar absorptance measurements were performed using an AZ Technology Model LPSR 300 instrument (0.3–2.5 μm range), again under active potentiostatic control.

***Calorimetric thermal vacuum measurements.*** "Thermal vacuum" in the space industry argot indicates a group of tests performed under space conditions with continuous cycling of the temperature as well as other parameters. "Calorimetric thermal vacuum" is a subset of this that uses thermal and heat flow analysis to directly measure the emittance or other relevant thermal properties of a material under space conditions, usually referencing a black body.[79–83]

In the present work, V-E electrochromic skins (devices) were affixed on their back side to a controllably heated Al plate (hot plate), placed near the top of the high vacuum chamber. A "cold plate" or "sink," also of Al, was placed below the hot Al plate assembly at some distance, near the bottom of the chamber. The entire apparatus was enveloped in a thermal shroud. The setup is shown schematically in Figure 1 and was based on an adaptation of a published[79] method.

The radiative transfer of heat from the hot to the cold Al plate, as modulated by the electrochromic device, was monitored by appropriately placed thermocouples. The emittance of the sample, $\varepsilon_s$, can then be given by the following equation (eq. 1), as described in more detail elsewhere.[79]

$$\varepsilon_s = \frac{VI}{\sigma A_s(\alpha_B T_s^4 - \varepsilon_B T_B^4)} \quad (1)$$

[Where: s= Stefan-Boltzmann constant ($5.67E^{-8}$ $Wm^{-2}K^{-4}$); αB = Solar absorptance of the blackbody (0.947); $\varepsilon_B$ = Emittance of blackbody (0.967); AS = Area of sample (0.0036m2 in our setup); V= Voltage supplied to device heater (volts); I = Current draw from device (i.e. V-E skin) heater (in amperes); $T_S$ = Average temperature of 4 thermocouples on back of device (in K); TB = Average temperature of 2 thermocouples on inside of black body cavity (in K).]

It may be noted that although $\alpha_B$ and $\varepsilon_B$ were both measured in our experiment, with values as noted above, in a perfect system $\alpha_B$ and $\varepsilon_B$ and are both = 1 and the above equation then simplifies to (eq. 2):

$$\varepsilon_s = \frac{VI}{\sigma A_s(T_s^4 - T_B^4)} \quad (2)$$

***Long-term space durability/stability tests.*** These were perfromed in a high vacuum bell jar equipped with multiple thermocouple and power feedthroughs. Devices (i.e., V-E skins) were actively electrochromically cycled (between extreme light/dark electrochromic states) periodically (typically every 1 h), while their temperature was also simultaneously cycled (between ca. −20 and +50°C), all while they were maintained in a vacuum of $10^{-6}$ to $10^{-7}$ Torr ($1.33 \times 10^{-4}$ to $10^{-5}$ Pa). This testing was performed continuously over periods of at least 4 months. Test results reported here are for a maximum 212-day (about 7 months) period.

***Calculation of spacecraft surface temperature from α(s) and ε values.*** Of utmost importance in space use of the V-E skins is to ensure that surface temperatures never exceed a particular value, usually about +90°C. The spacecraft surface temperature can be computed[29–31,77–82] for measured values of α(s) and ε, using a simple thermal calculation: now the heat, $q$, generated on direct exposure to solar radiation in space is given by (eq. 3):

$$q = (1350\,W/m^2[\text{solar constant}])\,X\,(\alpha(s)\,X\,(A[\text{area of device}])) \quad (3)$$

However, this quantity is also given by (eq. 4):

$$q(\text{rad}) = (F[\text{Boltzmann constant}])\,X\,(\varepsilon)\,(A)\,(Td^4 [\text{temperature of device or surface}]) - Ts^4[\text{space temperature, which is taken as } 4^oK] \quad (4)$$

Equating the two and solving for $T_d$, one arrives at (eq. 5):

$$T_d = [(1350/5.67X10^{-8})\,X\,(\text{Alpha(s)}/\varepsilon) + 256]^{1/4} \quad (5)$$

where, again, $T_d$ = device (V-E skin) surface temperature.

***Vacuum ultraviolet (VUV) exposure tests.*** These were performed under space conditions (including vacuum of $10^{-6}$ to $10^{-7}$ Torr [$1.33 \times 10^{-4}$ to $10^{-5}$ Pa]) using a Hamamatsu L2D2 Long-nose projecting type deuterium (UV) lamp with $MgF_2$ window powered by a Hamamatsu deuterium lamp C9598 power supply. The intensity (irradiance) of the lamp was $3.39 \times 10^{-4}$ W/cm$^2$ at a distance of 1 m, to be compared with the AM0 (Air Mass 0) solar intensity of $1.04 \times 10^{-5}$ W/cm$^2$. Thus, our UV lamp, at a distance of 1 m, had an intensity of 6.16 suns. Now our samples were placed at a distance of 7 cm from the lamp, which, from a simple calculation, yields an intensity of 819 suns at the surface of the V-E skin samples. Two exposure periods were used: 144 and 72 h, corresponding, respectively, to 14 and 7 years of typical space exposure, that is, equivalent sun hours (ESH).

***Electrostatic discharge (ESD) tests.***[82–84] These were performed in the laboratories of the Materials Physics Group of Utah State University (USU-MPG), Salt Lake City, UT (headed by Prof. J.R. Dennison), using induced electrostatic breakdown and surface voltage decay methodology and using USU-MPG's *in situ* electrostatic field probe (flipper). Observations were done of ESD and luminescence intensity and extent for three incident electron beams (2, 7, and 20 keV) at two incident fluxes (0.1 and 1.0 nA/cm$^2$). Detection included electrometer measurements and photodetection, as well as observations of surface damage. Measurements were then done of surface voltage (charge buildup) at selected incident electron beams (2, 7, and

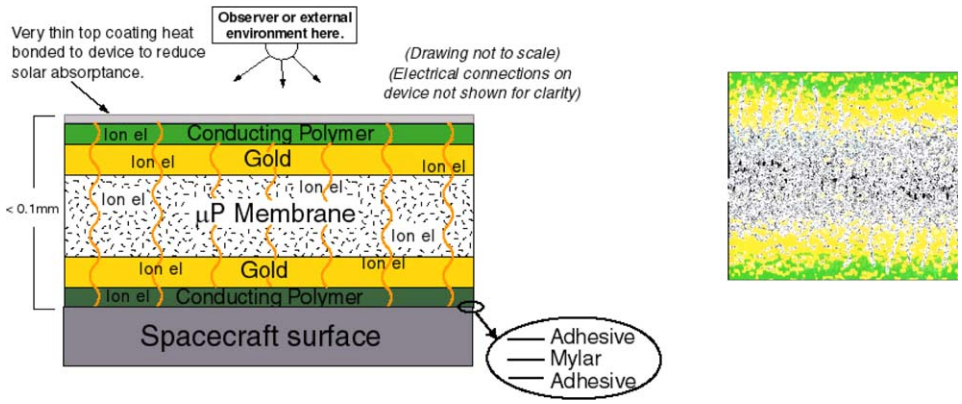


**Figure 2.** Left: Schematic diagram of the V-E skin. Right: Detail showing that the Au and CP layers are also "porous" and fibrillar in nature, rather than solid surfaces (as in the schematic at left). [Color figure can be viewed in the online issue, which is available at wileyonlinelibrary.com.]

20 keV) and incident fluxes (0.1 and 1.0 nA/cm$^2$) as well as selected applied voltage, and of incremental charging and charge dissipation after charging. Analyses were done of charge-discharge curves, conductivity, RIC of discharge, ESD strength, luminosity intensity, and energy/current thresholds. The relevant test specifications include MIL-STD 462, NASA-TP2361 (surface charging avoidance), NASA-HDBK-4002 (avoiding problems caused by spacecraft on-orbit internal charging effects), ASTM D-257/D-991 (surface resistivity), ASTM F 365-73T (shield testing), ASTM D-4238 (ESD), and AATCC 134-1979 (tribocharging).

***Atomic-oxygen exposure test.***[85–87] These were done at NASA Glenn Research Center (Cleveland, OH) under the direction of Dr Bruce Banks. The atomic-O fluence applied was $2.74 \times 10^{21}$ atoms/cm$^2$ (at a pressure of $10^{-6}$ Torr). This is in fact far greater (by more than an order of magnitude) than the typical fluence encountered by spacecraft: For example, the total fluence experienced by the European retrievable carrier (EURECA) spacecraft during 11 months of spaceflight was $2.3 \times 10^{20}$ atoms/cm$^2$.[86,87]

***Other tests.*** Vibration, acoustic, and shock testing was performed at various external labs (Gaynes Labs, Bridgeview, IL; Intertek Labs, Bridgewater, NJ; WRDC, Chaska, MN; Taber Industries, n. Tonawanda, NY) using published, mostly standard American Society for Testing and Materials (ASTM) methods (detailed descriptions of all the American Society for Testing and Materials [ASTM] tests quoted by name in this communication [including ASTM D4060] are available on the ASTM website and details of related tests of the International Standards Organization, ISO, Geneva, Switzerland can be found on that organization's website),[88–90] supplemented by those listed in the US military standard MIL-STD-1540.[88–90] Some of the detail of these tests[88–90] may be briefly provided here: acoustic, vibrational, shock. Acoustic: frequency ranges typically from 30 to 10,000 Hz. Vibrational: frequency ranges typically from 10 to 1500 Hz also including random vibration. Shock: pyrotechnical and electrical. Energy spectrum usually concentrated at or above 500 Hz and measured in frequency range of 100–10,000 Hz.

## RESULTS AND DISCUSSION

### Variable-Emittance (V-E) Skin Construction and Function

**Skin Construction.** Figure 2 shows a schematic diagram of the variable-emittance (V-E) skin (device), which comprises a single-membrane, 2-electrode system. The top layer of the skin comprises the substantially IR-transparent PE, directly heat-bonded to the working electrode surface, on which is deposited a well-adhering coating; this coating is also IR-transparent and is composed of doped-Ge, ITO, and other components as described in the Experimental Section. The function of this coating is to keep the $\alpha$(s) of the device <about 0.4, that is, it is the $\alpha$(s)-reduction-coating. Immediately below and directly heat-bonded to this top, PE layer is the active electrochromic CP surface, that is, the working electrode, deposited on one (the "front") side of the microporous membrane. Below this CP layer is the IR-reflective Au layer; Au is selected due to the fact that it possesses the highest IR reflectance of any metal across about 2.5–40 μm IR region of interest and is chemically inert to the constituents of the skins. The Au layer sits on the microporous membrane saturated with IonEl, followed by another Au layer on the "backside" of this membrane; this in turn is followed, finally, by a CP layer. This backside CP layer, which is about 5× as thick as the CP layer of the working (front or top) electrode, is part of the counter electrode. This backside CP layer in turn contacts a very thin (ca. 1 mil, 25 μm) sheet of Mylar® [poly(ethylene terephthalate)], to which it is bonded, along its perimeter, using a space-qualified, pressure-sensitive adhesive such as 3M Company 966.

Several features of this skin design allow for highly efficient, reflectance-mode, IR-electrochromic, and V-E function, and these are now briefly discussed: first, the working electrode, which is the active electrochromic surface, sees the incoming light beam directly, with no intervening material (such as electrolyte), other than the IR-transparent top surface; this is because the counter electrode is placed behind the working electrode. Second, the counter electrode is composed of a thicker film of the same CP as that of the working electrode. This allows for very high electrochemical reversibility, and thus electrochromic efficiency, since the redox reaction occurring at the

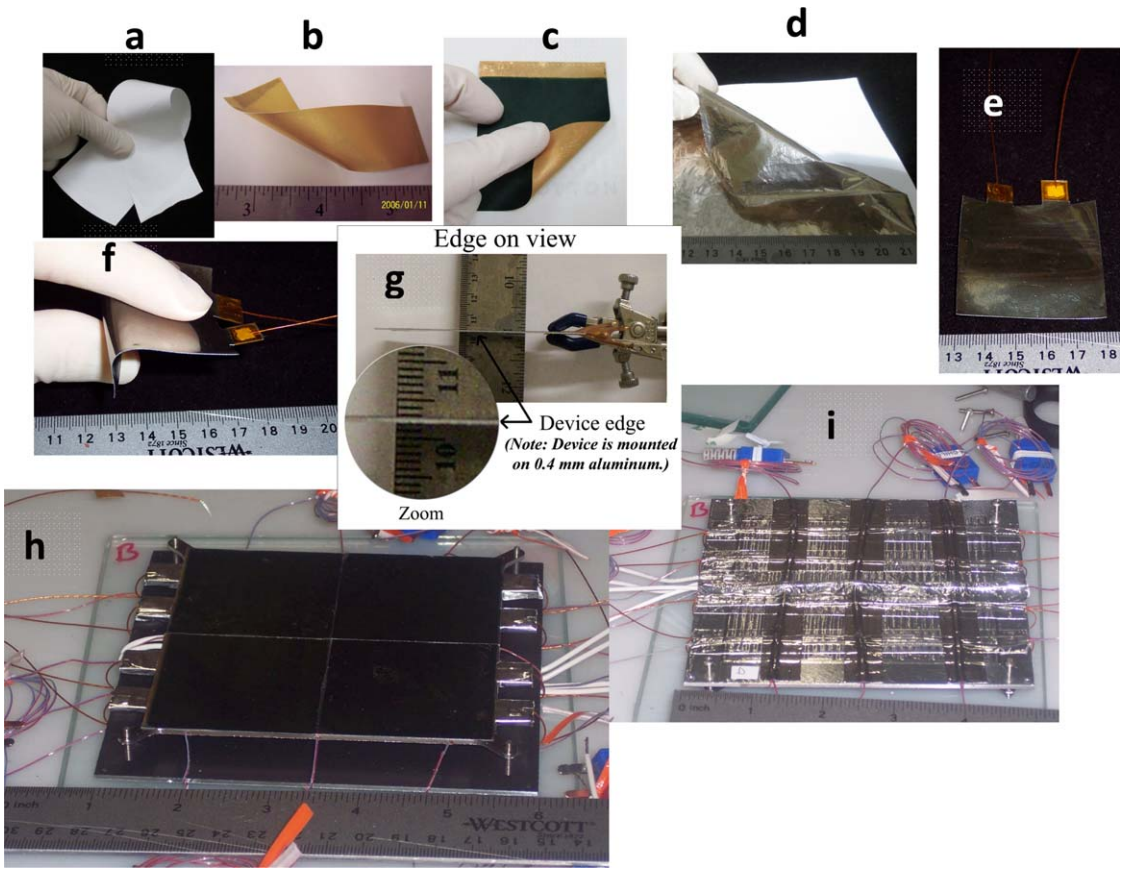


**Figure 3.** (a–d): Several major components of the skins: (a) Polysulfone microporous membrane. (b) Same, coated with Au on both sides. (c) Coated with CP (dark green) on one side. (d) Semiconductor-on-polyethyelene coating for $\alpha$(s) reduction. (e–g) Fully assembled skins (devices), one shown flexed and another edge-on, displaying extreme thinness. (h) Al test panel with four devices mounted on it, a typical test panel as used for space tests. (i) Same, obverse, showing heater coils used to test emittance performance. [Color figure can be viewed in the online issue, which is available at wileyonlinelibrary.com.]

counter electrode is the opposite of that occurring at the working electrode, and, due the 5× thickness of the CP therein, is not rate limiting. This is in contrast, for example, to many electrochromic systems, even those with "complimentarily coloring counter electrodes" where the electrochromics on the working and counter electrodes are different.[49–58] Third, a single-membrane system allows for electrolyte (IonEl) containment within the microporous membrane, yielding better integrity of the skins with greater flexibility and less "moving parts." Fourth, the direct heat-bonding of the PE top layer to the CP surface that comprises the active electrochromic prevents the permeation of electrolyte (IonEl) onto this CP surface; such permeated electrolyte would otherwise impede the IR signal, and hence the emittance performance, of the skins, since the IonEl is IR-absorptive. Finally, it is also noted that the use of a very thin polyester piece (<25 μm thick Mylar®) at the bottom, between the skin and the substrate (the spacecraft surface), allows for minimal impediment to heat transfer from the substrate, through the skin, to the external environment.

The constitution of the membrane with Au and CP deposited on it is not that of solid layers (CP/Au/μP) depicted in the main schematic in Figure 2, but rather that of a porous permeation of the Au and the CP into the body of the fibrous microporous membrane, as depicted at right in this Figure. This microporosity is critical to the permeation of the electrolyte (IonEl) into the CP, and thus the operation of the electrochromic device. The microporous membrane is selected for features such as compatibility with the IonEl used, compatibility with Au deposition, and appropriate poresize. A poresize of 0.05–0.5 μm is found ideal; too small a poresize leads to pore blockage on Au coating, and too large a poresize leads, on occasion, to discontinuous Au islands and, generally, to lack of significant electrochromism. The membrane also must possess sufficient thickness that the Au coatings on either side do not short out with each other, and must possess appropriate hydrophobicity/hydrophilicity properties and compatibility with the IonEl. Polysulfone and polycarbonate membranes are found to possess the most suitable properties in all these respects.

Figure 3 shows photos of: several major components of the skins; fully assembled skins (denoted "devices" for convenience), in various stages of flexure, showing excellent flexibility; the skin edge-on, showing extreme thinness; and an Al test panel containing four devices, a typical test panel as used for space-qualification tests. The skin remains extremely thin, flexible,

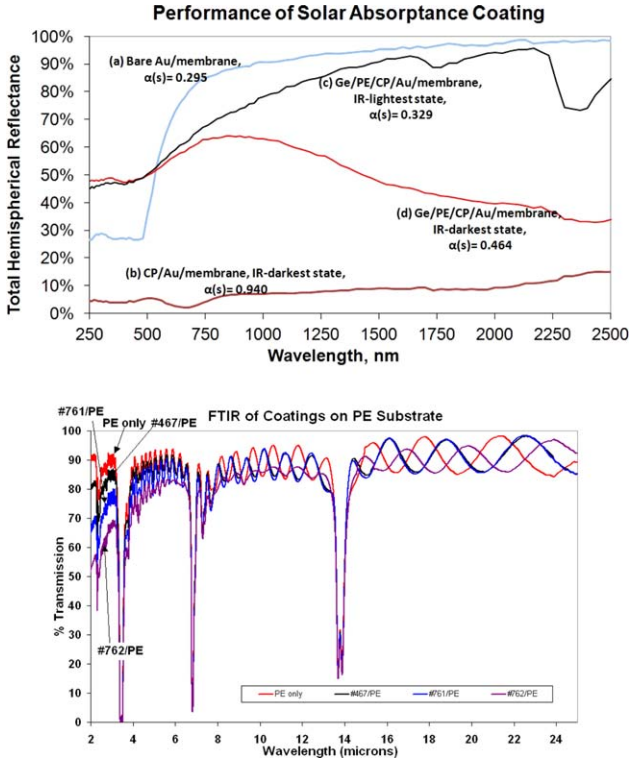


**Figure 4.** Top: Representative data for α(s)-reducing semiconductor coatings as incorporated into V-E skins (note that "Ge" is used generically for the entire semiconductor composition, which includes dopants and an ITO underlayer if applicable). Bottom: FTIR specular reflectance data for these coatings on PE (red—PE only; others—semiconductor coatings on PE, designated with various numbers, e.g., #762). The limited, narrow IR absorptions at about 3.5, 6.8, and 14 μm are due to PE. [Color figure can be viewed in the online issue, which is available at wileyonlinelibrary.com.]

and durable, and also cuttable with scissors to any size/shape (prior to final assembly). It can, if desired, be physically warped and otherwise abused with no observable damage or degradation in performance, although it is not likely to be during use as a V-E material.

***Skin operation.*** In operation, light corresponding to the IR spectral region (ca. 2.5–45 μm) passes through the top layer of the skin comprising the solar-reflective semiconductor coating and the PE, both of which are nearly completely IR-transparent, and impacts the CP. The CP then modulates the reflection of this light from the Au surface underlying it. In its reduced form (at ca. (−)1.0 V applied potential), the CP is substantially transparent in the IR, and the light passes through it and is reflected by the underlying Au surface back into the environment. In its partially oxidized form, at about (+)0.5 V applied potential, the CP is substantially IR-opaque, and the IR light is thus not reflected by the underlying Au surface. At applied voltages between these two limits, the IR light is reflected partially. Conversely, when light corresponding to the solar spectrum (with major components in the near-UV, visible, and NIR spectral regions, about 0.25–1.5 μm) is incident on the skin surface, it is primarily reflected by the solar-reflective semiconductor coating, regardless of the redox state of the underlying CP. Thus, in this manner, the skin exhibits V-E behavior, with emittance values from <0.11 to >0.90, while simultaneously holding its solar absorptance steady within a narrow range, typically 0.29–0.50.

***α(s)-reduction coating.*** We note at the outset that the fabrication of semiconductor coatings on flexible surfaces that have good adhesion and properties of IR-transparency combined with reflection of a substantial part of the solar spectrum has been exceedingly difficult and met with very limited success in extensive prior work heretofore.[75–78]

In our work as reported here, we successfully deposited very well-adhering coatings of doped-Ge with an underlying layer of extremely thin ITO on the "flexible outer layer" (PE) of the V-E devices, as described in detail in the Experimental Section. The thickness of the underlying ITO was kept between about 7 and 10 nm. Thinner ITO coatings yielded conductivity inadequate for acceptable anti-ESD properties and thicker coatings, requiring longer times in the vacuum deposition chamber, which invariably led to melting and deformation of the PE. It was next found that a Ge coating of thickness 30–55 nm and doped as needed with Si, Sn, and Te, applied on top of the ITO coating, yielded ideal IR-transparency combined with the lowest solar absorptance. The PE coated thus, that is, with doped-Ge/ITO, possessed a silvery, metallic appearance (Figure 3). Adhesion of the coatings on the PE was excellent. The composition of the final semiconductor coatings on PE were arrived at after more than 2 years of painstaking effort, with many failed coatings and burned-through PE substrates encountered on the way. Finding the right conditions for good adhesion on the PE was particularly laborious. This semiconductor coating, which drastically reduced the α(s) of the V-E devices, was one of the key breakthroughs in the V-E technology, allowing for its successful implementation.

Figure 4, top, shows representative reflectance and solar absorptance [α(s)] data for these α(s)-reducing semiconductor coatings as incorporated into V-E skins. The α(s) values are those measured by the solar absorptometer from the spectra shown. It is seen, first, that the α(s) of the skin incorporating the semiconductor/PE layer in its IR-lightest state, 0.329, is nearly that of the bare Au/microporous membrane substrate (0.295), which would possess the lowest α(s) possible in such V-E materials. Second, it is seen that on the other electrochromic extreme, that is, the IR-darkest state, while the α(s) of a bare skin (i.e., without a top Ge/PE layer with the active CP surface exposed to the external environment) is very high, 0.940, that of the same skin with the Ge/PE coating is reduced to just 0.464, which is excellent for space use. Figure 4, bottom, shows FTIR specular reflectance data for these coatings on PE, illustrating their extreme transparency in the entire IR region of thermal interest (the strong but extremely narrow absorptions due to the PE are also seen, at ca. 3.5, 6.8, and 14 μm).

***Ionic liquid electrolytes.*** Ionic liquids, which are essentially organic "room temperature molten salts," have found use in varied fields, from synthetic organic chemistry to drug delivery, to nanotechnology, and Li batteries.[60–66] Their utility for the present use, that is, for operation under extreme space vacuum and temperature conditions, lies in: (1) their wide "liquidus" range, that is, temperature range in which they remain liquid,

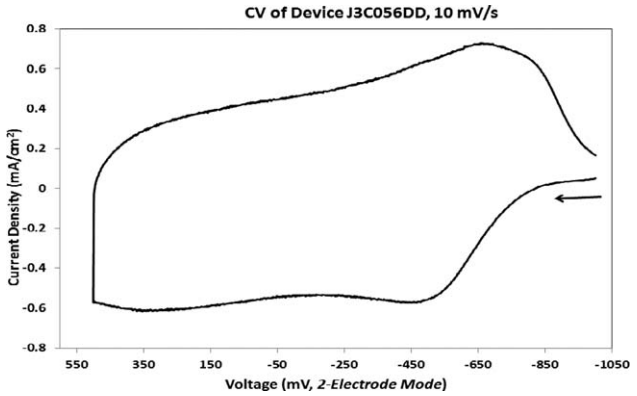


**Figure 5.** CV behavior of a typical V-E skin.

typically at least (−)40 to (+)100°C. (2) Their negligible vapor pressure: no observable evaporation in space vacuum over months; thus, no hermetic seal is required for our V-E skins using IonEls, in contrast to our earlier-generation V-E devices. (3) Their appreciable conductivity.

The two IonEls identified in the Experimental Section (together with added $LiBF_4$ salt) were selected based on an exhaustive screening and experimental study of 23 IonEls and four IonEl combinations, that is, for a total of 27 different compositions. The criteria used for selection included (1)-(3) listed above and in addition, (4) chemical compatibility with the microporous membranes used, and (5) cost. Of these 27 IonEls and combinations, 17 were eliminated in a prescreening based on their published physical, chemical, and other properties. These included (Im = imidazolium, other abbreviations standard): 1He-3Me-Im $BF_4$; 1Bu-3MeIm $PF_6$; 1He-3MeIm $PF_6$; 1Bu-3Me pyridinium bis(trifluoromethyl sulfonyl) imide; 1Bu-4Me pyridinium $PF_6$; 1Bu-4Me pyridinium $BF_4$; 1Bu-1Me pyrrolidinium $BF_4$; 1He-3MeIm triflate; 1Bu-3Me pyrazolium BETI; triMe-*n*-propyl ammonium bis(trifluoromethane sulfonyl) imide; *N*-methyl-*N*-propyl pyrolidinium bis(trifluoromethane sulfonyl) imide; bis(-pentafluoroethylsulfonyl) imide; 3Me-1Propyl Pyridinium bis(-trifluoro methylsulfonyl) imide; triMe pyrazolium Me sulfate; 1Et-3MeIm $PF_6$; 1Bu-3MeIm dicyanamide; and 1-Me-3-Octyl Im $BF_4$. Six IonEls were identified for testing in actual V-E skins, based on the criteria above: *n*-butylmethyl imidazolium tetrafluoroborate (BMIM-$BF_4$ or "BB"); 1-(2-hydroxyethyl)−3-methylimidazolium bis(trifluoromethylsulfonyl)imide (HEMIM-BTFOI or "NTF2"); 1Bu-3-Me-Imidazolium Triflate; 1Et-3-Me-Imidazolium $BF_4$; 1Bu-3MeIm-trifluoroacetate; 1Bu-1Me pyrrolidinium bis(trifluoro methyl sulfonyl) imide. Of these six, four additional 50 : 50 v/v combinations were made, yielding 10 candidates to be tested in V-E skins. The two finally selected yielded the best performance in terms of delta emittance, switching time, space durability, and related parameters.

In spite of these beneficial properties, their practical use in our V-E skins was not trivial. It was not a simple question of replacing the earlier electrolyte with them; V-E skins fabricated by such replacement simply did not function. Rather, a complex charging procedure had to be used, as described at length in the Experimental Section. Additionally, after charging with the IonEls, the skins further required a complex "activation" procedure, arrived at after painstaking trial and error, to work. In this regard, our work may be contrasted with that of other work incorporating IonEls with CP-based electrochromic devices, mostly with solid, nonporous ITO/Mylar electrodes[67–71]; all of this prior work pertains to the visible–NIR rather than the IR region, and none has, to the best of published knowledge, been thus far deployed in any functional systems.[67–71]

As noted above, in total, 27 IonEls were tested in our work, individually and in various combinations and with and without additional salt additives. The formulation described in the Experimental Section is the best found (in terms of V-E device performance). Although the conductivity of the IonEls (even with salt additives as in our work) falls significantly at temperatures < about (−)10°C, affecting the switching time of the V-E devices, this was overcome with relatively simple artifices, primarily the application of overvoltages for switching at lower temperatures, as described in more detail below.

### IR-Electrochromic and V-E (Including Thermal Vacuum) Performance

Figure 5 shows the CV of a typical V-E skin incorporating a poly(aniline) (PANI)-based CP matrix and the optimized IonEl, between the voltages used to generate the extreme IR-light and IR-dark states, which are (−)1.0 and (+)0.5 V, respectively (in 2-electrode mode). We have described this behavior in our earlier communications.[2,12–18,24–29] Very briefly, at −1.0 V, the CP is in its completely reduced, nonconductive, IR-transparent and substantially visible–NIR-transparent, leuco-emeraldine form. Following the first anodic oxidation peak, at about 0.0 V, the CP is in its conductive, doped-emeraldine form; in this form, bipolaronic states lead to its highest IR absorption. On further oxidation (not shown in the Figure 5) at about +0.8 V, the CP is in its nonconductive, pernigraniline form, at which it is highly opaque in the visible–NIR region, but at the same time, substantially IR-transparent again, a phenomenon discussed at length elsewhere.[2,12–18,24–29]

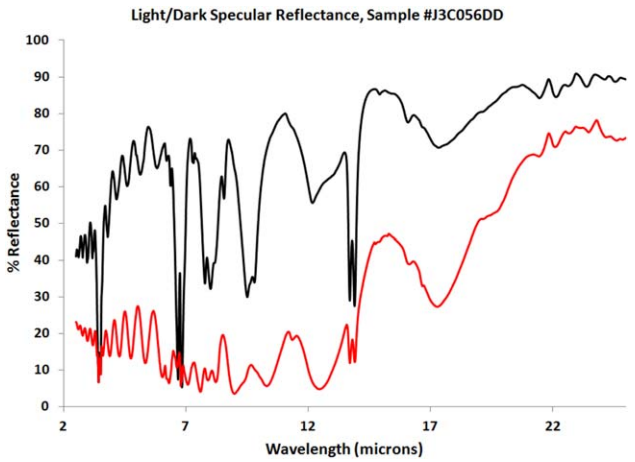


**Figure 6.** Typical IR electrochromic contrast of the V-E skins, represented as specular reflectance FTIR (16° incidence angle) in IR-light (black) and IR-dark (red) states (again, the sharp absorptions at ca. 3.5, 6.8, and 14 μm are due to PE). [Color figure can be viewed in the online issue, which is available at wileyonlinelibrary.com.]

**Table I.** Summary Data of Emissometer-Based Emittance Measurements for Various V-E Skins ("Devices")

| Device (sample) # | Light $\varepsilon$ | Dark $\varepsilon$ | $\Delta\varepsilon$ |
|---|---|---|---|
| Skins with alpha(s)-reduction coating | | | |
| J3C056DD | 0.325 | 0.771 | 0.446 |
| J3A038FD | 0.298 | 0.784 | 0.486 |
| J3A038CD | 0.234 | 0.676 | 0.442 |
| J3A174BD | 0.389 | 0.646 | 0.427 |
| Skins without alpha(s)-reduction coating | | | |
| JB_011AD | 0.257 | 0.771 | 0.514 |
| JB_042AD | 0.237 | 0.751 | 0.514 |
| JA_168FD | 0.335 | 0.835 | 0.500 |

Those with and without the $\alpha$(s)-reduction coating are compared, to demonstrate the (minimal) effect of this coating on emittance function

Figure 6 shows typical IR electrochromic contrast of the skins, represented as specular reflectance FTIR (16° incidence angle) in IR-light and IR-dark states (again, the sharp absorptions at ca. 3.5, 6.8, and 14 μm are due to PE). It is to be noted that in these skins, the light/dark reflectance difference, that is, delta reflectance, remains substantially the same while the "window," that is, the absolute value of the reflectance, can be shifted up or down to a substantial degree. For example, referring to Figure 5, at about 9 μm, the high/low reflectance values for device J3C056DD are 71.8 and 4.3%, respectively, with a delta reflectance of 67.5%; these can be shifted to, for example, 78.8% and 12.3%, yielding a more IR-reflective device while maintaining the delta reflectance at 67.5%. It is also to be noted that these V-E skins, incorporating the solar-reflective, semiconductor/PE layer, showed, by design, minimal variation in the visible–NIR spectral region, corresponding to their solar absorptance behavior.

Emittance measurements were performed using both the emissometer, for ambient-pressure measurements, and calorimetric thermal vacuum techniques,[79–83] emulating space conditions (including space vacuum), as described in the Experimental Section. Table I summarizes emissometer-based emittance measurements for various V-E devices (skins). Devices with and without the $\alpha$(s)-reduction coating are compared, to demonstrate the (minimal) effect of this coating on emittance function. First listed is an optimized device carrying the optimized $\alpha$(s)-reduction coating; this shows an emittance variation of 0.325–0.771, for a delta emittance of 0.446. Next listed in this table are emittance data for slightly lighter and darker skins, showing that the "window-shift" seen in the FTIR reflectance data, as discussed above, can be replicated in the emittance data. Finally listed are data for two devices without the top, $\alpha$(s)-reduction coating. These show considerably higher delta emittance (>0.500 and up to 0.514, as seen); this indicates that the top $\alpha$(s)-reduction coating does have a very slight, detrimental effect on the emittance performance of the electrochromic skins. All these data show that the emittance performance of these latest-generation V-E skins, especially as measured by delta emittance and switching time, is considerably superior to that of prior-generation electrochromic devices that we have reported on previously.[2,12–18,24–29]

**Table II.** Comparison of Emittance Measurements Using the Emissometer (At Ambient Pressure) and the Calorimetric Thermal Vacuum (CalTVac) Method (in space vacuum), For a Representative Device (Skin), # J3D155AD

| Light $\varepsilon$ | Dark $\varepsilon$ | $\Delta\varepsilon$ |
|---|---|---|
| Measurements with emissometer (at ambient pressure) | | |
| 0.376 | 0.777 | 0.401 |
| Measurements with CalTVac (in space vacuum) | | |
| 0.376 | 0.730 | 0.354 |

**Table III.** Calculation of Spacecraft Skin Surface Temperature from Measured $\alpha$(s) and $\varepsilon$ Values of a Typical Device (Per Treatment Given in Experimental Section)

| | Light state | Intermediate state $\varepsilon$ | Dark state $\Delta\varepsilon$ |
|---|---|---|---|
| $\alpha$(s) | 0.306 | 0.342 | 0.434 |
| $\varepsilon$ | 0.383 | 0.589 | 0.841 |
| $\alpha$(s)/$\varepsilon$ | 0.799 | 0.581 | 0.516 |
| Skin Temp ($T_d$), K | 371.4 | 342.9 | 332.9 |
| Skin Temp ($T_d$), °C | 98.2 | 69.7 | 59.8 |

Figure 7 shows typical switching of the V-E skins, measured as an emittance variation; the rapid switching time seen, about 6 to 9 s, is in fact not required for spacecraft use, where switching times of up to 30 s or more are adequate.[8–11,24–29] The data in Figure 7 allow for a simple calculation of the coloration and bleaching switching times at 95% of maximum transmittance, a property useful for appreciation of how fast these V-E skins switch. Now, from the figure, the light (bleached) state and dark (colored) state %$R$ values are 54.8% and 19.4%, respectively, yielding a delta%-reflectance of 35.5%. Taking the first dark-to-light (i.e., colored to bleached) transition, we have 108.77 s (at 19.4%) to 124.52 s (at 53.1%, which is 95% of the maximum transmittance) = 15.8 s for the dark to light (colored to bleached) switching time. Similarly, for the light-to-dark transition, we have 172.05 s (at 54.9%) to 185.6 s (at 21.2%, which is 95% of the total light-to-dark transition) = 13.6 s for the light to dark (bleached to colored) switching time.

The emissometer data were supplemented by calorimetric thermal vacuum (CalTVac) emittance data (Experimental Section). The CalTVac data represent a more realistic assessment of performance in space, since they are performed in space vacuum (ca. $10^{-7}$ Torr, $10^{-5}$ Pa) and emulate conditions of thermal cycling (Experimental Section). Table II shows representative emittance data for a representative device using this (CalTVac) method. The table also lists, for comparison, emittance data for the same device measured using the emissometer. It is seen that the CalTVac $\Delta\varepsilon$ values, measured in space vacuum, are about 10% lower than those measured using the emissometer at ambient (atmospheric) pressure. This is expected behavior, ascribed to the fact that the IonEl has poorer access to the CP in the microporous membrane in space vacuum, due to the absence of

**Table IV.** Space Durability/Stability Data for V-E Devices (Skins) Subject to Continuous Electrochromic (Light/Dark) Cycling While also Thermally Cycled Between ca. About −20 and +50 °C, all in Space Vacuum ($10^{-7}$ Torr, $10^{-5}$ Pa), for a Period of 212 Days (ca. 7 months)

| | ε's, Pre-Test | | | ε's, Post-Test, 64 days | | | ε's, Post-Test, 212 days | | |
|---|---|---|---|---|---|---|---|---|---|
| Sample # | Light ε | Dark ε | Δε | Light ε | Dark ε | Δε | Light ε | Dark ε | Δε |
| J3A056AD | 0.363 | 0.720 | 0.357 | 0.397 | 0.724 | 0.327 | 0.420 | 0.747 | 0.327 |
| J3A056ED | 0.249 | 0.613 | 0.364 | 0.241 | 0.587 | 0.346 | 0.291 | 0.648 | 0.357 |

a surface pressure confining it; we have observed this elsewhere as well.[59,72,73]

Of utmost importance in space use of the V-E skins is to ensure that surface temperatures never exceed a particular value, usually about +100°C. The spacecraft surface temperature can be computed for given, measured values of α(s) and ε, using a simple thermal calculation, as per the discussion and equations presented in the Experimental Section. Such a calculation for a representative device is summarized in Table III. These data show that the key parameter determining the temperature is the ratio, α(s)/ε. Furthermore, they show, counter-intuitively, that the dark (high-emittance) state of the V-E skin actually leads to the coolest surface temperatures (59.8°C). That is to say, when facing the sun, it is best to be in the dark, high-emittance, electrochromic state rather than the light electrochromic state. The results in Table IV also show that, with the use of the α(s)-reduction coating, the surface temperature of the V-E skin, and thus the spacecraft, is very significantly lowered, to a maximum of <100°C, the approximate threshold level for effective functioning of the spacecraft. This may be compared to the case without any such coating, where similar calculations show that unacceptable temperatures of >200°C are generated. In the dark state, the skin is an excellent thermal emitter, and emits its excess heat efficiently into space.

## Space Durability and Function Under Space Conditions

**Long-Term Performance Under Space Conditions.** As described in the Experimental Section, to test space durability and stability, V-E devices (skins) were subject to continuous electrochromic (light/dark) cycling while also thermally cycled between about −20 and +50°C, all in space vacuum ($10^{-7}$ Torr, $10^{-5}$ Pa). Table IV shows representative results of these tests, up to a period of 212 days (ca. 7 months). It is to be noted that the devices (skins) given in the table were of "mediocre" emittance performance. Their excellent durability and stability over the period tested (212 days) are nevertheless clearly seen in the data.

***Function at low temperatures.*** As noted above, the conductivity of the IonEls (even with salt additives as in our work) falls significantly at temperatures below about (−)10°C, affecting the switching of the V-E devices, especially *in vacuo*, where the effect of the vacuum also plays a part (see above). The lowered conductivity in turn affects the performance of the V-E skins, seen not only in a much longer (up to 3×) switching time, but also in slightly poorer emittance performance. This effect was overcome with a relatively simple method: application of overvoltages when switching at lower temperatures *in vacuo*. At the low temperatures and in space vacuum, the use of such overvoltages was not found to degrade the CP, for reasons discussed earlier. A "calibration curve" or "lookup table" for required overvoltages was generated, which listed the actual voltage needed to be applied to a device, at a particular, low temperature in space vacuum, to achieve the same emittance (mean of

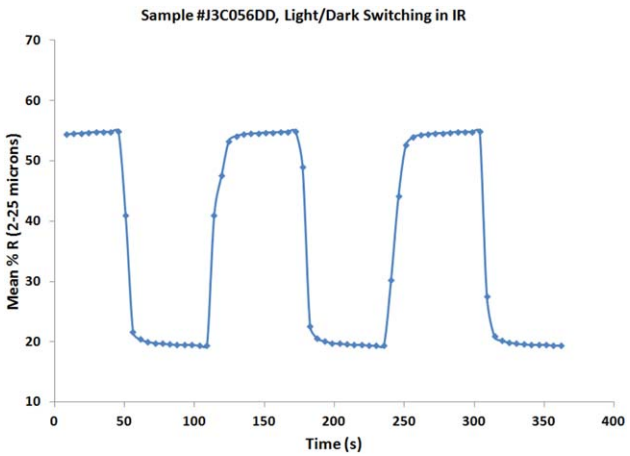


**Figure 7.** Typical switching of the V-E skins, measured as %*R* (specular reflectance, 16° incidence angle) variation. (see Experimental Section for method of data collection). [Color figure can be viewed in the online issue, which is available at wileyonlinelibrary.com.]

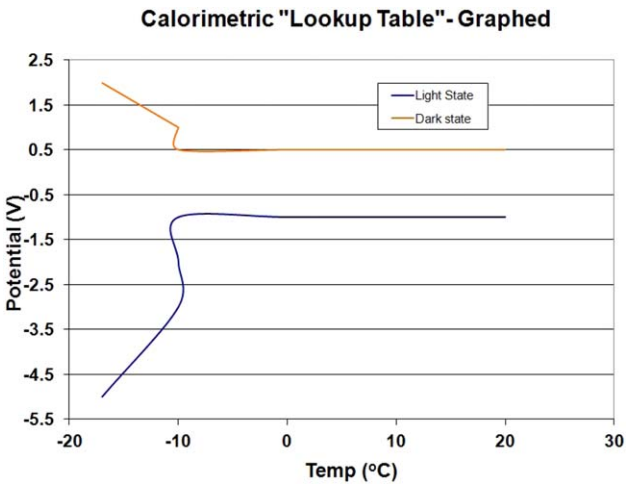


**Figure 8.** "Calibration curve" or "lookup table," depicted graphically, showing the actual voltage needed to be applied to a device at lower temperatures in space vacuum, to achieve the same emittance as achieved at room temperature, for IR-light (low emittance) and IR-dark (high emittance) states (see text for detailed discussion). [Color figure can be viewed in the online issue, which is available at wileyonlinelibrary.com.]

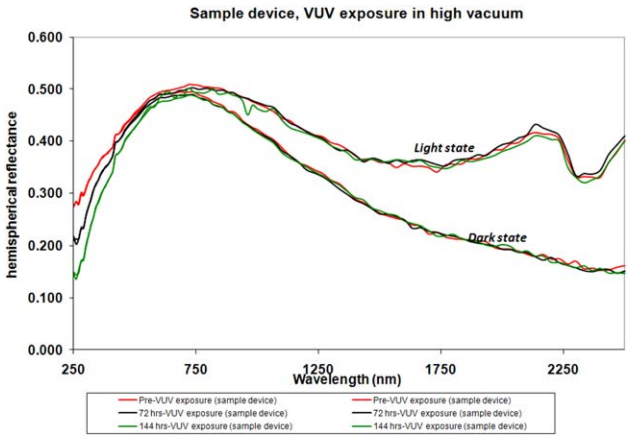


**Figure 9.** Summary results from VUV exposure of V-E skins (reflectance spectra corresponding to the spectral region of the solar spectrum), for exposure periods corresponding to 14 years of typical space exposure. [Color figure can be viewed in the online issue, which is available at wileyonlinelibrary.com.]

emissometer and thermal vacuum measurements) as achieved at room temperature with the "standard" voltages [(+)0.5 and (−)1.0 V for IR-dark (high emittance) and IR-light (low emittance) states, respectively]. This "lookup table" is depicted graphically in Figure 8. It is seen that at temperatures of (−)20°C, substantial overvoltages, about (−)5.0 and (+)1.75 V for the light and dark states, respectively, were needed to be applied.

***Other space/environmental durability tests.*** As noted in the Experimental Section, the V-E skin samples tested under VUV in space vacuum were exposed to an equivalent intensity of 819 suns at their surface.[79–83] Two exposure periods were used: 144 and 72 h, corresponding respectively, to 14 and 7 years of typical space exposure, that is, ESH. Data are summarized in Figure 9. It is clearly seen that there is no degradation observed at all, in the spectral region corresponding to the solar spectrum.

The V-E skins also passed the extensive ESD tests[81–84] (see Experimental Section, detailed results omitted for space reasons). Passing the ESD test was indicated as <5% deterioration in emittance and solar absorptance function after versus before the test. The V-E skins also passed the atomic-O (A-O) exposure tests,[85–87] which, as noted in the Experimental Section, used A-O fluences that were one order of magnitude higher than the highest found in low-earth orbit and geosynchronous orbit.[86,87] Among other means of recording A-O results, before/after photographs were used. Representative data are shown in Figure 10. The V-E skins also passed standard[79–83] micrometeoroid and solar wind tests. Finally, the V-E skins also passed several other environmental durability tests not relevant to space performance, but rather to handling and shelf-life durability, including, for example, the ASTM D4060 abrasion test.[88–90] All these tests were interpreted in a "pass/fail" fashion, and the V-E skins passed all tests. The voluminous data from these tests are not listed in this communication for space reasons.

## CONCLUSIONS

In this article, we have introduced the second generation of variable-emittance (V-E) IR electrochromics based on CPs, microporous membranes, and IonEls, for application in efficient spacecraft thermal control. Such thermal control is an essential if uncelebrated requirement for all spacecraft. These electrochromics are now deployable in actual spacecraft. They overcome the space durability and space functionality problems of a first generation of V-E materials, we reported on earlier.[2,12–18,24–28,45–48] These drawbacks are overcome with several breakthrough developments, which involve use of: (1) unique IonEls, imparting space durability. (2) IR-transparent, solar-reflective semiconductor coatings that drastically lower the solar absorptance [$\alpha(s)$], while leaving the emittance ($\varepsilon$) properties unaffected. (3) Single-membrane substrates with working electrode (active electrochromic CP) and counter electrode (also CP) on opposite sides of a single microporous membrane, yielding extremely thin (<0.3 mm), flexible V-E skins that can be cut with scissors to any size/shape. (4) Removal of electrochromically inactive material from the CP matrix, using unique techniques, to greatly enhance V-E performance. The incorporation of the IonEls with the electrochromic CPs is nontrivial and requires the use of specially developed charging and activation techniques before the IonEls function well with the CPs. Data presented show tailorable emittance ($\varepsilon$) variations from 0.19 to 0.90 and $\Delta\varepsilon$ values of >0.50, the highest reported thus far for any functional V-E material, to our knowledge. These may be compared with the $\Delta\varepsilon > 0.40$ threshold required for efficient

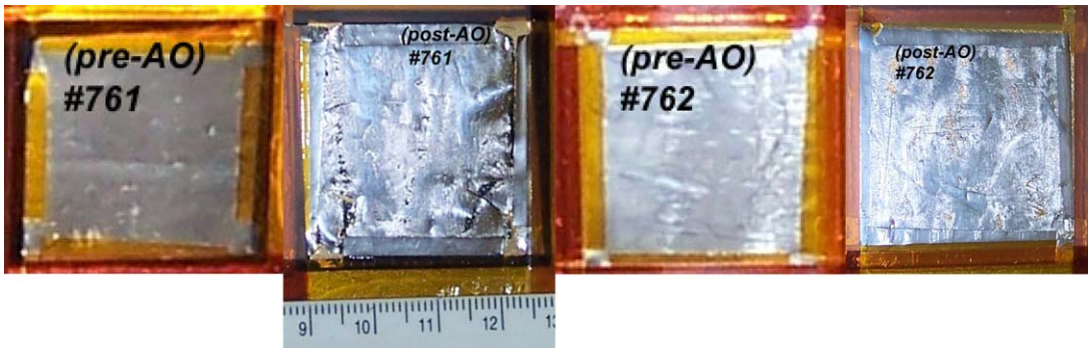


**Figure 10.** Representative atomic-O (A-O) exposure test results. Shown are pre- and post-A-O-exposure photos of V-E devices. Numbers shown are sample numbers (see text for discussion). [Color figure can be viewed in the online issue, which is available at wileyonlinelibrary.com.]

spacecraft thermal control. High/low emittance switching times of 6–9 s are reported, to be again compared with the 30 s considered adequate for space use. These values are measured both with emissometer and industry-standard calorimetric thermal vacuum techniques. It is noted that these are the highest reported $\Delta\varepsilon$ values for any functional V-E material, to the best of published knowledge,[33–44] this is in spite of attempts to use our prior work[2,12–18,24–28,45–48] as a basis to improve on emittance performance of thin film V-E materials, for example, as done by Li et al.[91] Space durability over more than 7 months under active electrochromic and temperature cycling in space vacuum ($<10^{-5}$ Pa) is demonstrated with minimal degradation. Durability to VUV, atomic-O exposure, micrometeoroids, and solar wind is also demonstrated. It is also noted that these advanced, applied polymers are now actively deployable in a specific application (spacecraft thermal control), and thus demonstrate more than just "potential" application. This very lightweight and inexpensive technology is the only V-E technology that will work with microspacegraft (<20 kg) and nanospacecraft (<2 kg; e.g., the nanosats),[19–23] thus eventually allowing for much greater flexibility in the design of these very small spacecraft. This has the potential to "democratize" the entire space industry, since even small firms would be in a position to launch their own, dedicated satellites without having to share satellite space and capabilities with larger firms.

## ACKNOWLEDGMENTS

Partial support of this work by the (U.S.) National Aeronautics and Space Administration (NASA) through Contract #s NNX12CA64C, NNX11CG21P, NNJ11HD02P, NNX09CA68C and NNX08CB96P to Ashwin-Ushas Corporation is gratefully acknowledged. The authors also thank the following for assistance: Dr. Gaj Birur, NASA-Jet Propulsion Laboratory, Pasadena, CA; Dr. Bruce Banks, NASA-Glenn Research Center, Dayton, OH; Mr. Dan Butler-NASA-Goddard Space Flight Center, Greenbelt, MD; Prof. J.R. Dennison, Materials Physics Group, Utah State University (USU-MPG), Salt Lake City, UT.

## REFERENCES

1. Schechter, E. Popular Mechanics, July 1, 2013. Available at: http://www.popularmechanics.com/technology/military/research/whatever-happened-to-counter-infrared-camouflage-15648261. Accessed on February 2014.
2. Chandrasekhar, P.; Zay, B. J.; Birur, G. C.; Rawal, S.; Pierson, E. A.; Kauder, L.; Swanson, T. *Adv. Funct. Mater.* **2002**, *12*, 95.
3. Yu, D.-B.; Tang, K.; Zou, J.-W.; Wand, Z.-R.; Wang, F.; Jiang, T. Infrared and Laser Engineering, 2007, 2007-2, TN219. Available at: http://en.cnki.com.cn/Article_en/CJFDTOTAL-HWYJ200702015.htm. Accessed on February 2014.
4. Wang, Y.-J.; Hu, J.-H.; LU, X.-L.; Li, L. Infrared Technology, 2008, 2008-06, TJ06. Available at: http://en.cnki.com.cn/Article_en/CJFDTOTAL-HWJS200806015.htm. Accessed on February 2014.
5. Chen, X.; Yang, L.; Xie, J. Opto-Electronic Engineering, 2007, 2007-01, TP391.9. Available at: http://en.cnki.com.cn/Article_en/CJFDTOTAL-GDGC200701010.htm. Accessed on February 2014.
6. Phan, L.; Walkup I. V.; W. G.; Ordinario, D. D.; Karshalev, E.; Jocson, J.-M.; Burke, A. M.; Gorodetsky, A. A. *Adv. Mater.* **2013**, *25*, 5621.
7. Proceedings of Defense Conference on Night Vision 2000, London, UK, March **2000**.
8. de Parolis, M. N.; Pinter-Krainer, W. European Space Agency Bulletin, 1996, 87. Available at: http://www.esa.int/esapub/bulletin/bullet87/paroli87.htm. Accessed on February 2014.
9. Gilmore, D. G., Ed. Spacecraft Thermal Control Handbook, Vol. *I*: Fundamental Technologies; American Institute of Aeronautics & Astronautics: Washington, DC, **2002**.
10. Meseguer, J.; Pérez-Grande, I.; Sanz-Andrés, A., Eds. Spacecraft Thermal Control; Woodhead Publishing: New York, **2012**.
11. Proceedings of Spacecraft Thermal Control Workshop, El Segundo, CA, March 26–28, **2013**. Available at: http://www.cvent.com/events/2013-spacecraft-thermal-control-workshop/event-summary-8f568c6257494feb93a2620988a7dc17.aspx. Accessed on February 2014.
12. Chandrasekhar, P.; Zay, B. J.; McQueeney, T. M.; Birur; G.; Sitaram, V.; Menon, R.; Elsenbaumer, R. L. *Synth. Met.* **2005**, *155*, 623.
13. Chandrasekhar, P.; Zay, B. J.; Ross, D. A.; McQueeney, T. M.; Birur; Swanson, T.; Kauder, L.; Douglas, D. In Chromogenic Phenomena in Polymers: Tunable Optical Properties (ACS Proceedings Volume); Jenekhe, S. A.; Kiserow, D. J., Eds.; American Chemical Society Symposium Series, 888, **2005**.
14. Chandrasekhar, P. In Introduction to Organic Electronic and Optoelectronic Materials and Devices; Sun, S.-S.; Dalton, L. R., Eds.; CRC Press: Boca Raton, **2008**; Chapter 23, p 713.
15. Chandrasekhar, P.; Naishadham, K. *Synth. Met.* **1999**, *105*, 115.
16. Chandrasekhar, P. Conducting Polymers: Fundamentals and Applications. A Practical Approach, with Foreword by Lawrence Dalton. Kluwer Academic Publishers: Dordrecht, **1999**; Chapter 3.
17. Yang, S. C.; Chandrasekhar, P. Optical and Photonic Applications of Electroactive and Conducting Polymers, Proceedings of the SPIE, The International Society for Optical Engineering, San Diego, CA, July 12–13, **1995**; SPIE Press: Bellingham, WA, 1995.
18. Sigma-Aldrich, Available at: at http:\\www.ashwin-ushas.com, under Electrochromics > Spacecraft Thermal Control. Accessed on February 2014.
19. Lockheed Martin Awarded Nanosatellite Contract, Available at: http://www.azonano.com/news.asp?newsID=2787. Accessed on February 2014.
20. NASA Ames Partners With M2MI For Small Satellite Development, Available at: http://www.nasa.gov/home/hqnews/2008/apr/HQ_08107_Ames_nanosat.html. Accessed on February 2014.

21. Cornell Wins A NASA Launch For Nano Satellite. Available at: http://cusat.cornell.edu/. Accessed on February 2014.
22. Cornell's CUSat Has Won the Nanosat-4 Flight Competition. Available at: http://www.spacemart.com/reports/Cornell_Wins_A_NASA_Launch_For_Nano_Satellite_999.html. Accessed on February 2014.
23. UTIAS/SFL arranged the launch of its first experimental nanosatellite, CanX-1. Available at: http://utias-sfl.net/?page_id=150. Accessed on February 2014.
24. Paris, A.; Anderson, K.; Zay, B.; McQueeney, T.; Chandrasekhar, P. Electrochromic Radiators for Microspacecraft Thermal Control, Proceedings of the 20th Annual Conference on Small Satellites, Logan, UT, USA VIII, 1, **2005**.
25. Chandrasekhar, P.; Zay, B. J.; McQueeney, T. M.; Ross, V. A.; Lovas, A.; Ponnappan, R.; Gerhart, C.; Swanson, T.; Kauder, L.; Douglas, D.; Peters, W.; Birur, G. Variable Emittance Materials Based on Conducting Polymers for Spacecraft Thermal Control, Proceedings of the Space Technology and Applications International Forum (STAIF-2003), Albuquerque, NM, USA, **2003**.
26. Chandrasekhar, P.; Zay, B. J.; McQueeney, T. M.; Scara, A.; Ross, D. A.; Birur; G.; Haapanen, S.; Kauder, L.; Swanson, T.; Douglas, D. *Synth. Met.* **2003**, *135*, 23.
27. Chandrasekhar, P.; Zay, B. J.; Ross, D. A.; McQueeney, T. M.; Birur, Swanson, T.; Kauder, L.; Douglas, D. *Polym. Prepr.* **2002**.
28. Chandrasekhar, P.; Birur, G. C.; Stevens, P.; Rawal, S.; Pierson, E. A.; Miller, K. L. *Synth. Met.* **2001**, *119*, 293.
29. Bannon, E. T.; Bower, C. E.; Sheth, R.; Stephan, R. Electrochromic Radiator Coupon Level Testing and Full Scale Thermal Math Modeling for Use on Altair Lunar Lander, paper presented at American Institute of Aeronautics and Astronautics (AIAA) annual meeting, 2010, on test results on Ashwin-Ushas' variable emittance electrochromics, **2010**.
30. Duffie, J. A.; Beckman, W. A. Solar Engineering of Thermal Processes, 2nd ed.; Wiley: New York, **1991**.
31. Siegel, R.; Howell, J. R. Thermal Radiation Heat Transfer; Taylor & Francis: New York, **2002**.
32. Schmieder, D. E.; Walker, G. W. The Infrared and Electro-Optics Systems Handbook; Acceta, J. S.; Shumaker, D. L., Eds.; SPIE Press: Bellingham, **1993**; Vol. *7*, p. 182.
33. Swanson, T. D. (NASA) US Pat. 6,538,796 B1, **2003**.
34. Marren, K. Microscopic Radiator Flying on "Skin" of a NASA Spacecraft, JHU Applied Physics Lab. Available at: http://www.jhuapl.edu/newscenter/pressreleases/2006/060313.asp. Accessed on February 2014.
35. Kruzelecky, R. V.; Haddad, E.; Wong, B.; Jamroz, W. R. US Pat. 7,761,053 B2, **2010**.
36. Braig, A.; Meisei, T.; Rothmund, W.; Braun, R. *J. Aerospace* **1994**, *1229*, 941465.
37. Wehner, J. W.; Harris, C. M.; O'Rell, M. K. US Pat. 7,219,860 B2, **2007**.
38. Cognata, T. J.; Leimkuehler, T. O.; Sheth, R. B.; Le, H. NASA-Johnson internal document, 2013.
39. Gregoire, D. J.; Kirby, D. J. US Pat. 8,017,217, **2011**.
40. Cumberland, R.; Carter, W. B. B.; Gross, A. F. US Pat. 7,691,284 B2, **2010**.
41. Friedman, M. H. US Pat. 7,390,123 B2, **2008**.
42. Kelliher, W. C.; Young, P. R. Investigation of Phase-Change Coatings for Variable Thermal Control of Spacecraft. Available from NASA, NASA Technical Note No. D-6756, June 1972.
43. Huchler, M.; Natusch, A.; Rothmund, W. SAE Technical Paper Series. Proceedings of the 25th International Conference on Environmental Systems, San Diego, CA, July 1995, 951674.
44. Demiryont, H. Variable emittance electrochromic device for satellite thermal control, AIP Conference Proceedings—Proceedings of the Space Technology and Applications International Forum (STAIF) 813, Springer-Verlag: New York, 2006.
45. Chandrasekhar, P. US Pat. 5,995,273, **1999**.
46. Chandrasekhar, P. Electrolytes, US Pat. 6,033,592, **2000**.
47. Chandrasekhar, P. Electrochromic Display Device, Can. Pat. 2,321,894, May 8, **2007**.
48. Chandrasekhar, P. Electrochromic Display Device, Eur. Pat. Appl. No. 99908208.4, April 17, **2009**.
49. da Silva, A. J. C.; Nogueira, F. A. R.; Tonholo, J.; Ribeiro, A. S. *Sol. Energy Mater. Sol. Cells* **2011**, *95*, 2255.
50. Sapp, S. A.; Sotzing, G. A.; Reynolds, J. R. *Chem. Mater.* **1998**, *10*, 2101.
51. Bhandari, S.; Deepa, M.; Pahal, S.; Joshi, A. G.; Srivastava, A. Kumar; Kant, R. *ChemSusChem* **2010**, *3*, 97.
52. Groenendaal, L.; Jonas, F.; Freitag, D.; Pielartzik, H.; Reynolds, J. R. *Adv. Mater.* **2000**, *12*, 481.
53. Reynolds, J. R.; Dyer, A. L.; Unur, E. US Pat. 8,284,473 B2, October 9, **2012**.
54. Schwendemann, I.; Hickman, R.; Soenmez, G.; Schottland, P.; Zong, K.; Welsh, D. M.; Reynolds, J. R. *Chem. Mater.* **2002**, *14*, 3118.
55. Reeves, B. D.; Thompson, B. C.; Abboud, K. A.; Smart, B. E.; Reynolds, J. R. *Adv. Mater.* **2002**, *14*, 717.
56. Franke, E. B.; Trimble, C. L.; Hale, J. S.; Schubert, M.; Woollam, J. A. Faculty Publications from the Department of Electrical Engineering, University of Nebraska, (http://digitalcommons.unl.edu/libraryscience/, accessed April 2014) **2000**.
57. Li, Z.; Zhang, Y.; Holt, A.; Kolasa, B. P.; Wehner, J. G.; Hampp, A.; Bazan, G. C.; Nguyen, T.-Q.; Morse, D. E. *New J. Chem.* **2011**, *35*, 1327.
58. Mortimer, R. *J. Ann. Rev. Mater. Res.* **2011**, *41*, 241.
59. Chandrasekhar, P. PCT/Int. Pat. Appl. No. PCT/US13/32320, March15, **2013**.
60. Ohno, H., Ed. Electrochemical Aspects of Ionic Liquids; Wiley: Hoboken, 2005.
61. Arnaud, C. A. Ionic Liquids Improve Separations, *Chem. Eng. News*, **2012**, *90*, 36.
62. Galinksi, M.; Lewandowski, A.; Stepniak, I. *Electrochim. Acta* **2006**, *51*, 5567.
63. Shin, J.-H.; Henderson, W. A.; Passerini, S. *Electrochem. Commun.* **2003**, *5*, 1016.

64. Gordon, C. M.; McCluskey, A. *Chem. Commun.* **1999**, 1431.
65. Dyson, P. J.; Ellis, D. J.; Parker, D. G.; Welton, T. *Chem. Commun.* **1999**, 25.
66. Mathews, C. J.; Smith, P. J.; Welton, T. *Chem. Commun.* **2000**, 1249.
67. Lu, W.; Fadeev, A. G.; Qi, B.; Smela, E.; Mattes, B. R.; Ding, J.; Spinks, G. M.; Mzurkiewicz, J.; Zhou, D.; Wallace, G. G.; MacFarlane, D. R.; Forsyth, S. A.; Forsyth, M. *Science* **2002**, *297*, 983.
68. Beaupre, S.; Dumas, J.; Leclerc, M. *Chem. Mater.* **2006**, *18*, 4011.
69. Lu, W.; Fadeev, A. G.; Qi, B.; Mattes, B. R. *J. Electrochem. Soc.* **2004**, *151*, H33.
70. Lu, W.; Mattes, B. R.; Fadeev, A. G. US Pat. 6,828,062, **2004**.
71. Lu, W.; Fadeev, A. G.; Qi, B.; Mattes, B. R. *Synth. Met.* **2003**, *135–136*, 139.
72. Chandrasekhar, P.; Pirgov, P.; Zay, B. J.; Lawrence, D.; Morefield, S.; Rittenhouse, T. L.; Clementi, S. G.; Truong, Q.; Greene, R. R. *Adv. Mater. Phys. Chem.* **2013**, *3*, 217.
73. Chandrasekhar, P. Functionalized-Conducting-Polymer-Microporous-Membrane Based Voltammetric Sensor Skins with High Selectivity/Sensitivity, Multiple Analyte Sensing in Single Interrogation, Wide Operating Temperature, Low Power, Technical Status Report M18 for Contract # W911QY-12-C-0032, to US Army Natick Soldier Research, Development and Engineering Center, Natick, MA, U.S. Defense Technical Information Center (DTIC): Washington, DC, October 15, **2013**.
74. Saito, Y.; Yamagami, T.; Matsuzaka, Y.; Namiki, M.; Ohta, S.; Toriumi, M.; Yokota, R.; Makino, F.; Matsumoto, T.; Hirosawa H. *Adv. Space Res.* **2002**, *30*, 1159.
75. Roth, J. A.; Hall, J. T.; Neal, D. G.; Wilkinson, C. R.; Lai, S.; Johnson, M. W. U.S. Pat. 7,270,891 B2, **2007**.
76. Biricik, V. W.; Rowe, J. M.; Kraatz, P.; Tully, W.; Thompson, W. J.; Modster, R. W. U.S. Pat. 5,173,443, **1992**.
77. Available at: http://wwwold.ece.utep.edu/research/webedl/cdte/Fabrication/index.htm. Accessed on February 2014.
78. Available at: http://www.cleanroom.byu.edu/processes.phtml. Accessed on February 2014.
79. Puterbaugh, R. L.; Mychkovsky, A. G.; Ponnappan, R.; Kislov, N. *AIP Conf. Proc.* **2005**, *746*, 90.
80. Welch, J. W. In Spacecraft Thermal Control Handbook: Fundamental Technologies, Chapter 19; Gilmore, D. G., Ed.; American Institute of Aeronautics and Astronautics (AIAA): Washington, DC, **2002**.
81. U.S. Air Force. Military Handbook: Application Guidelines for MIL=STD-1540B: Test Requirements for Space Vehicles (MIL-HDBK-340); U.S. Air Force, **1985**.
82. Perl, E.; Do, T.; Peterson, A.; Welch, J. Environmental Testing for Launch and Space Vehicles, The Aerospace Corporation, 2005. Available at http://www.aero.org/publications/crosslink/fall2005/02.html. Accessed on February 2014.
83. Newell, J. N.; Man, K. F. Environmental Testing of MEMS for Space Applications; NASA-JPL Publication, **1998**.
84. Smith, W. C. U.S. Pat. 4,885,543, **1989**.
85. de Groh, K. K.; Banks, B. A. *J. Spacecr Rockets* **2006**, *43*, 414.
86. Banks, B. A.; Demko, R. Atomic Oxygen Protection of Materials in Low Earth Orbit, NASA Document No. NASA/TM-2002–211360, February, 2002. Available at: http://ntrs.nasa.gov/archive/nasa/casi.ntrs.nasa.gov/20020038835_2002060999.pdf. Accessed on February 2014.
87. IBEX spacecraft images the heliotail, revealing an unexpected structure, e! Science News, July 10, 2013. Available at: http://esciencenews.com/articles/2013/07/10/ibex.spacecraft.images.heliotail.revealing.unexpected.structure. Accessed on February 2014.
88. American Society for Testing and Materials (ASTM). Available at: http://www.astm.org/Standard/index.shtml. Accessed on February 2014.
89. International Standards Organization, ISO, Geneva, Switzerland. Available at: http://www.iso.org/iso/home.html. Accessed on February 2014.
90. MIL-STD-1540 Department of Defense Standard Practice. Product Verification Requirements for Launch, Upper Stage, and Space Vehicles, 1999. Available at: http://snebulos.mit.edu/projects/reference/MIL-STD/MIL-STD-1540D.pdf. Accessed on February 2014.
91. Li, H.; Xie, K.; Pan, Y.; Yao, M.; Xin, C. *Synth. Met.* **2009**, *159*, 1386.